J|A|C|S
ARTICLES
Published on Web 12/11/2007

Small Au and Pt Clusters at the Anatase TiO_2(101) Surface: Behavior at Terraces, Steps, and Surface Oxygen Vacancies

Xue-Qing Gong,*,†,§ Annabella Selloni,† Olga Dulub,‡ Peter Jacobson,‡ and Ulrike Diebold*,‡

Department of Chemistry, Princeton University, Princeton, New Jersey 08544, and Department of Physics, Tulane University, New Orleans, Louisiana 70118

Received September 21, 2007; E-mail: xgong@ecust.edu.cn; diebold@tulane.edu

Abstract: The adsorption properties of Au and Pt metal nanoclusters on TiO_2 anatase (101) were calculated using density functional theory. Structures and energetics of adsorbed Au and Pt monomers, dimers, and trimers at clean anatase TiO_2(101) terraces and two major step edges, as well as O-vacancies, were systematically determined. The theoretical predictions were tested by vapor-depositing small coverages of Au and Pt on anatase (101) and investigating the resulting clusters with Scanning Tunneling Microscopy. On the clean surface, Au shows a strong tendency to form large clusters that nucleate on step edges. A preference for adsorption at type D-(112) steps is observed, which is probably a result of kinetic effects. For Pt, clusters as small as monomers are observed on the terraces, in agreement with the predicted large binding energy of 2.2 eV. Step edges play a less important role than in the case of Au. Oxygen vacancies, produced by electron irradiation, dramatically influence the growth of Au, while the nucleation behavior of Pt was found to be less affected.

1. Introduction

Model catalysts in the form of metal clusters supported on well ordered metal oxide surfaces can provide important insights into the properties and behavior of real catalysts and have thus attracted a great deal of attention over the past decade.[1−4] In these model systems, the interaction between the metal cluster and the support has a crucial role both in the nucleation and initial growth of the metal and in the geometric and electronic structure of the resulting cluster/oxide interface, which in turn has a strong influence on the catalytic activity.[5−9]

In this paper we focus on the interaction of small Au and Pt clusters with the (101) surface of the anatase polymorph of titanium dioxide (TiO_2). TiO_2 is a versatile oxide material with important applications in many fields,[10] and as a support for metal clusters, it is often found to promote their catalytic activity.[11,12] In this respect, platinum is one of the most studied metals on single-crystal TiO_2 surfaces, and Pt/TiO_2 is the prototypical SMSI (strong metal−support interaction) system.[10] Similarly, gold nanoparticles supported on TiO_2 surfaces have been extensively investigated in recent years for their applications as catalysts for low-temperature CO oxidation, selective propene oxidation, and other catalytic and photocatalytic oxidation reactions.[9−11,13−18] Among the various TiO_2 polymorphs, rutile, and especially its (110) surface, is the most widely used in surface science studies.[10] On the other hand, anatase is of particular interest in photocatalysis,[19,20] and noble metals like Au and especially Pt are often employed to enhance its photocatalytic efficiency.[19] The (101) surface is the most stable termination of anatase.[21] Scanning Tunneling Microscopy (STM) studies of this surface show the presence of numerous monoatomic-height steps and a variety of point defects, including surface oxygen vacancies and various not well-identified surface and subsurface impurities. These step and defect sites are expected to have an important influence on the interaction of the anatase (101) surface with metal clusters.

For rutile TiO_2(110), numerous investigations have addressed the role of surface defects on the structural, electronic, and catalytic properties of deposited metal particles (see, e.g., refs

† Princeton University.
‡ Tulane University.
§ Present address: Research Institute of Industrial Catalysis, East China University of Science and Technology, 130 Meilong Road, Shanghai 200237, P. R. China.

(1) Campbell, C. T. *Surf. Sci. Rep.* **1997**, *27*, 1.
(2) Goodman, D. W. *Chem. Rev.* **1995**, *95*, 523.
(3) Henry, C. R. *Surf. Sci. Rep.* **1998**, *31*, 231.
(4) Baumer, M.; Freund, H. J. *Prog. Surf. Sci.* **1999**, *61*, 127.
(5) Haruta, M. *Chem. Rec.* **2003**, *3*, 75.
(6) Nakajima, H.; Mori, T.; Watanabe, M. *J. Appl. Phys.* **2004**, *96*, 925.
(7) Subramanian, V.; Wolf, E. E.; Kamat, P. V. *J. Am. Chem. Soc.* **2004**, *126*, 4943.
(8) Schwartz, V.; Mullins, D. R.; Yan, W. F.; Chen, B.; Dai, S.; Overbury, S. H. *J. Phys. Chem. B* **2004**, *108*, 15782.
(9) Chen, M. S.; Goodman, D. W. *Catal. Today* **2006**, *111*, 22.
(10) Diebold, U. *Surf. Sci. Rep.* **2003**, *48*, 53.
(11) Haruta, M. *Catal. Today* **1997**, *36*, 153.
(12) Valden, M.; Lai, X.; Goodman, D. W. *Science* **1998**, *281*, 1647.
(13) Panagiotopoulou, P.; Kondarides, D. I. *J. Catal.* **2004**, *225*, 327.
(14) Panagiotopoulou, P.; Christodoulakis, A.; Kondarides, D. I.; Boghosian, S. *J. Catal.* **2006**, *240*, 114.
(15) Iida, H.; Kondo, K.; Igarashi, A. *Catal. Commun.* **2006**, *7*, 240.
(16) Iida, H.; Igarashi, A. *Appl. Catal., A* **2006**, *298*, 152.
(17) Boccuzzi, F.; Chiorino, A.; Manzoli, M.; Andreeva, D.; Tabakova, T. *J. Catal.* **1999**, *188*, 176.
(18) Sakurai, H.; Ueda, A.; Kobayashi, T.; Haruta, M. *Chem. Commun.* **1997**, 271.
(19) Linsebigler, A. L.; Lu, G. Q.; Yates, J. T., Jr. *Chem. Rev.* **1995**, *95*, 735.
(20) Thompson, T. L.; Yates, J. T., Jr. *Top. Catal.* **2005**, *35*, 197.
(21) Diebold, U.; Ruzycki, N.; Herman, G. S.; Selloni, A. *Catal. Today* **2003**, *85*, 93.

 10.1021/ja0773148 CCC: $40.75 **© 2008 American Chemical Society**

7−9, 22−40). By contrast, studies of metal particles on well-defined anatase surfaces are scarce.[41−44] The purpose of this work is to understand the role of different surface sites, specifically terraces, step edges, and oxygen vacancies, in the nucleation and growth of small Au and Pt clusters on anatase TiO_2(101). Experimentally, metals on oxide substrates are usually deposited by evaporation. The key steps in the growth are the nucleation, corresponding to the adsorption of a single metal atom, and the formation of a critical size cluster, i.e., a cluster whose size can only grow or remain constant.[45,46] In many cases the critical size cluster is simply a dimer or sometimes a trimer. To get insights into the nucleation and initial growth of Pt and Au on anatase, we have performed a comparative study of the adsorption of Pt and Au monomers (Pt_1 and Au_1), dimers (Pt_2 and Au_2), and trimers (Pt_3 and Au_3) at terraces, step edges, and O-vacancies on the anatase TiO_2-(101) surface. For step edges, we rely on the structures that we have recently analyzed in detail by STM measurements and DFT calculations.[47] The theoretical predictions were tested by evaporating small coverages of Au and Pt on clean anatase (101) and on surfaces that were first irradiated with electrons to produce oxygen vacancies.[48] The preferred adsorption sites of the resulting small clusters were analyzed with Scanning Tunneling Microscopy (STM). When trying to compare total-energy calculations with experiments, one has to keep in mind that kinetic effects can prevent lowest-energy configurations to form and lead to kinetically limited structures.[49] Within this caveat, the experimental results agree well with the theoretical predictions.

2. Computational and Experimental Details

2.1. Calculations. The total energy DFT calculations have been carried out within the generalized gradient approximation (GGA) using the PWScf code included in the Quantum-Espresso package.[50] Electron-ion interactions were described by ultrasoft pseudopotentials,[51] with electrons from Pt and Au 5d, 6s; O 2s, 2p; and Ti 3d, 4s shells explicitly included in the calculations. Plane-wave basis set cutoffs for the smooth part of the wavefunctions and the augmented density were 25 and 200 Ry, respectively. The anatase TiO_2(101) surface was modeled as a periodic slab with six layers of oxide, and the vacuum between slabs is ∼10 Å. A (2 × 2) surface cell with a corresponding 2 × 2 × 1 *k*-point mesh was used. Steps were modeled using appropriate vicinal surfaces. In particular, we considered the vicinal anatase TiO_2(134) and TiO_2(301) surfaces for the steps denoted D-(112) and B-(100) (see below), respectively. We used a (1 × 2) surface cell together with a 2 × 3 × 1 *k*-point mesh to study the adsorption of metal clusters on the vicinal TiO_2(301) surface. For monomer adsorption on anatase TiO_2-(134), we employed a (1 × 1) surface cell with a corresponding 2 × 3 × 1 *k*-point mesh, while, for dimer and trimer adsorption, we used a twice as large (1 × 2) surface cell with a 2 × 2 × 1 *k*-point mesh, in order to avoid interaction between clusters in neighboring cells. To model the reduced TiO_2(101) surface, we created a surface O-vacancy by removing one bridging oxygen in either a (2 × 2) or (3 × 2) surface cell. These cells were then used to study the adsorption of the metal clusters. In all cases, the clusters were adsorbed on one side of the slab only. During structural optimization, all the atoms of the slab and clusters were allowed to relax, except those on the outmost layer on the clean side of anatase TiO_2(101). The force threshold for the optimization was 0.05 eV/Å.

To estimate the adsorption energies, two different expressions were considered[42,43]

$$E^{\mathrm{ads}}_{\mathrm{M}_n} = -\left(E_{\mathrm{M}_n/\mathrm{TiO}_2} - E_{\mathrm{TiO}_2} - E_{\mathrm{M}_n}\right)$$

$$E^{\mathrm{coh}}_{\mathrm{M}_n} = -(E_{\mathrm{M}_n/\mathrm{TiO}_2} - E_{\mathrm{TiO}_2} - nE_{\mathrm{M}})/n$$

in which E_{M_n}/TiO_2 is the total energy of the interacting M_n metal cluster + TiO_2 support; E_{TiO_2} is the total energy of the clean TiO_2 slab; E_{M_n} is the total energy of the metal cluster in its most stable gas-phase conformation;[42,52] and E_M is the total energy of a single metal atom. Clearly, $E^{\mathrm{ads}}_{\mathrm{M}_n} = E^{\mathrm{coh}}_{\mathrm{M}_n}$ for $n = 1$; for dimers and trimers, $E^{\mathrm{ads}}_{\mathrm{M}_n}$ represents the adsorption (or desorption) energy of the cluster as a whole while $E^{\mathrm{coh}}_{\mathrm{M}_n}$ is the average adsorption energy per atom.

2.2. Experimental Details. The experiments were carried out in an ultrahigh vacuum (UHV) chamber (base pressure of less than 1×10^{-10} mbar) equipped with experimental facilities for low-energy electron diffraction (LEED) and scanning tunneling microscopy (STM). The anatase single crystal, a natural mineral sample, was cleaned *in situ* by repeated cycles of Ar^+ ion bombardment (1 keV) at room temperature and annealing at 800−900 K. Surface cleanliness was probed with X-ray photoelectron spectroscopy (XPS) in a separate UHV chamber. A well-defined (1 × 1) LEED pattern was observed on the clean surface. The STM experiments were carried out using an Omicron UHV-STM-1 at room temperature. All STM images were recorded in constant current mode at a positive sample bias in the range 1 to 2.2 V and with feedback currents between 0.3 and 3 nA. Electrochemically etched W tips, cleaned by argon sputtering and by applying voltage pulses during operation, were used in the STM.

Electron irradiation was performed with a thoroughly outgassed low-energy electron gun. The electron beam was rastered across the surface with a current density of $\sim 7.7 \times 10^{13}$ electrons/cm^2·s and had an

(22) Parker, S. C.; Campbell, C. T. *Top. Catal.* **2007**, *44*, 3.
(23) Matthey, D.; Wang, J. G.; Wendt, S.; Matthiesen, J.; Schaub, R.; Laegsgaard, E.; Hammer, B.; Besenbacher, F. *Science* **2007**, *315*, 1692.
(24) Yang, Z. X.; Wu, R. Q.; Goodman, D. W. *Phys. Rev. B* **2000**, *61*, 14066.
(25) Yang, Z. X.; Wu, R. Q. *Phys. Rev. B* **2003**, *67*, 081403.
(26) Pillay, D.; Hwang, G. S. *Phys. Rev. B* **2005**, *72*, 205422.
(27) Lopez, N.; Norskov, J. K. *Surf. Sci.* **2002**, *515*, 175.
(28) Iddir, H.; Öğüt, S.; Browning, N. D.; Disko, M. M. *Phys. Rev. B* **2005**, *72*, 081407.
(29) Okazaki, K.; Morikawa, Y.; Tanaka, S.; Tanaka, K.; Kohyama, M. *Phys. Rev. B* **2004**, *69*, 235404.
(30) Chretien, S.; Metiu, H. *J. Chem. Phys.* **2007**, *127*, 084704.
(31) Liu, Z. P.; Hu, P.; Alavi, A. *J. Am. Chem. Soc.* **2002**, *124*, 14770.
(32) Wahlstrom, E.; Lopez, N.; Schaub, R.; Thostrup, P.; Ronnau, A.; Africh, C.; Laegsgaard, E.; Norskov, J. K.; Besenbacher, F. *Phys. Rev. Lett.* **2003**, *90*, 026101.
(33) Liu, Z. P.; Gong, X. Q.; Kohanoff, J.; Sanchez, C.; Hu, P. *Phys. Rev. Lett.* **2003**, *91*, 266102.
(34) Molina, L. M.; Rasmussen, M. D.; Hammer, B. *J. Chem. Phys.* **2004**, *120*, 7673.
(35) Remediakis, I. N.; Lopez, N.; Norskov, J. K. *Angew. Chem., Int. Ed.* **2005**, *44*, 1824.
(36) Moreau, F.; Bond, G. C. *Appl. Catal., A* **2006**, *302*, 110.
(37) Iliev, V.; Tomova, D.; Bilyarska, L.; Eliyas, A.; Petrov, L. *Appl. Catal., B* **2006**, *63*, 266.
(38) Sun, B.; Vorontsov, A. V.; Smirniotis, P. G. *Langmuir* **2003**, *19*, 3151.
(39) Chen, M. S.; Goodman, D. W. *Science* **2004**, *306*, 252.
(40) Yan, W. F.; Chen, B.; Mahurin, S. M.; Schwartz, V.; Mullins, D. R.; Lupini, A. R.; Pennycook, S. J.; Dai, S.; Overbury, S. H. *J. Phys. Chem. B* **2005**, *109*, 10676.
(41) El-Azab, A.; Gan, S.; Liang, Y. *Surf. Sci.* **2002**, *506*, 93.
(42) Vittadini, A.; Selloni, A. *J. Chem. Phys.* **2002**, *117*, 353.
(43) Han, Y.; Liu, C. J.; Ge, Q. F. *J. Phys. Chem. B* **2006**, *110*, 7463.
(44) Iddir, H.; Skavysh, V.; Ogut, S.; Browning, N. D.; Disko, M. M. *Phys. Rev. B* **2006**, *73*, 041403(R).
(45) Brune, H. *Surf. Sci. Rep.* **1998**, *31*, 121.
(46) Venables, J. A. *Introduction to Surface and Thin Film Processes*; Cambridge University Press: 2000.
(47) Gong, X. Q.; Selloni, A.; Batzill, M.; Diebold, U. *Nat. Mater.* **2006**, *5*, 665.
(48) Dulub, O.; Batzilln, M.; Solovev, S.; Loginova, E.; Alchagirov, A.; Madey, T. E.; Diebold, U. *Science* **2007**, *317*, 1052.
(49) Katsiev, K.; Batzill, M.; Diebold, U.; Urban, A.; Meyer, B. *Phys. Rev. Lett.* **2007**, *98*, 186102.
(50) Baroni, S.; De Gironcoli, S.; Dal Corso, A.; Giannozzi, P. Quantum-Espresso, http://www.democritos.it.
(51) Vanderbilt, D. *Phys. Rev. B* **1990**, *41*, 7892.
(52) Xiao, L.; Wang, L. C. *J. Phys. Chem. A* **2004**, *108*, 8605.

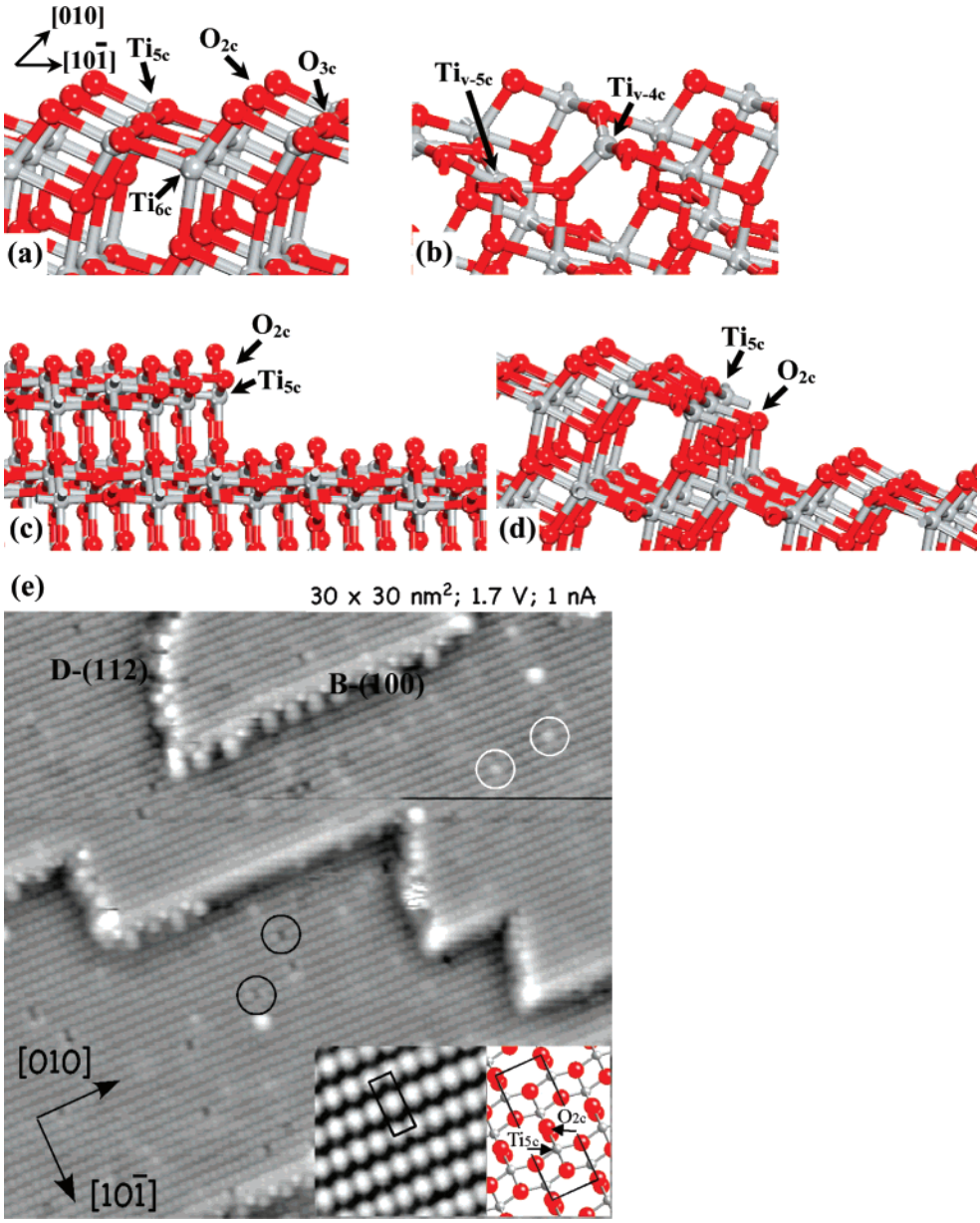

Figure 1. Calculated structures of (a) clean terrace, (b) O vacancy, (c) step D-(112), and (d) step B-(100) at anatase TiO_2(101) surfaces. The Ti atoms are in gray, and O, in red. This notation is used throughout this paper. (e) STM image of a clean anatase (101) surface with the atomically resolved structure shown in the inset. The bright protrusions located on the bright O_{2c} rows indicated by white circles are tentatively assigned to hydroxyl groups, and the dark features indicated by black circles are probably impurities.

electron energy of 300 eV. Pt and Au were vapor-deposited on the well-ordered (sputtered and annealed) and e-irradiated anatase (101) surfaces at room temperature. The pressure during metal deposition remained below 6×10^{-10} mbar in the UHV chamber. The deposition rates of Pt and Au were 8×10^{-5} Å·s^{-1} and 4×10^{-4} Å·s^{-1}, respectively. The deposition rates of both metals were initially calibrated with a quartz-crystal microbalance and cross-checked by depositing small amounts of both metals on a rutile TiO_2(011) crystal, which is easier to handle experimentally than anatase (101). Quoted coverages are based on a statistical analysis of cluster densities and heights measured with STM. The height of the clusters on the terraces was measured from the top of each cluster's cross sectional profile to its base; for clusters at the step edges their height was measured to the lower terrace. The width of the clusters was measured on the cluster's profile cross-section at mid-height level taking STM tip convolution effect into account. The concentration of deposited Pt is given in monolayer equivalents (ML), which corresponds to a Pt(111) packing density of 1.5×10^{15} Pt atoms per cm^2 and an Au(111) packing density of 1.39×10^{15} Au atoms per cm^2.

3. Results

3.1. Anatase TiO_2(101): Terraces, Steps, and Oxygen Vacancies. The anatase TiO_2(101) surface (see Figure 1a) exposes both fully saturated 3(6)-fold O(Ti), $O_{3c}(Ti_{6c})$, and coordinatively unsaturated (cus) 2(5)-fold O(Ti), $O_{2c}(Ti_{5c})$, atoms. In the optimized structure, O_{2c} (O_{3c}) atoms are displaced inward (outward) by ~0.08 (~0.2) Å with respect to their bulk-truncated positions, while Ti_{5c} (Ti_{6c}) atoms are displaced inward (outward) by ~0.15 (~0.2) Å.[53] The partially reduced surface (Figure 1b) was modeled by removing a bridging O_{2c} atom from a (2×2) surface supercell (vacancy coverage = 1/4 ML). This

(53) Lazzeri, M.; Vittadini, A.; Selloni, A. *Phys. Rev. B* **2001**, *63*, 155409.

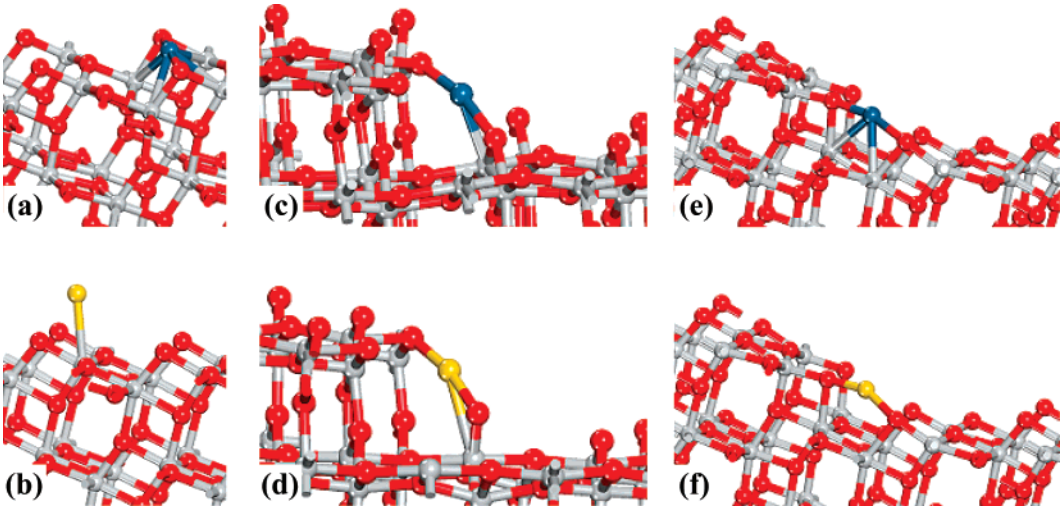

Figure 2. Calculated structures of adsorbed Pt/Au monomers at (a)/(b) terraces, (c)/(d) step D-(112), and (e)/(f) step B-(100) of anatase TiO_2(101) surfaces. The Pt atoms are dark blue, and Au atoms are yellow.

was found to have a formation energy of 4.81 eV (evaluated with respect to O_2 in the gas phase) and gives rise to important local structural relaxations: the neighboring Ti_{6c} and Ti_{5c} atoms, which become five- and fourfold Ti (Ti_{v-5c} and Ti_{v-4c}), respectively, are relaxed inward by ~0.2 Å, while the exposed subsurface O_{3c} is relaxed outward by ~0.2 Å. Test calculations using a (2 × 3) surface cell gave very similar results both for the relaxed structure and for the vacancy formation energy (4.71 eV, 1/6 ML). The structure and energetics of steps on anatase (101) have been described in detail recently.[47] The two most stable steps, shown in Figure 1c and d, expose undercoordinated Ti_{5c} and O_{2c} atoms, similarly to the (101) terraces. The step in Figure 1c, whose computed formation energy is 0.04 eV/Å, occurs at the two nonparallel sides of the characteristic trapezoidal islands on the (101) surface. It exposes a TiO_2(112) facet and will be called D-(112). The step in Figure 1d, with a formation energy of 0.10 eV/Å, is the longer of the two parallel sides of the islands. It exposes the low-index anatase TiO_2(100) facet and will be called B-(100).

Figure 1e shows an experimental STM image of the clean surface prior to metal deposition. In empty-states STM images O_{2c} are typically observed as bright atoms, with an elliptical shape slightly elongated toward the neighboring Ti_{5c}. The exact appearance of atomically resolved STM images is a strong function of bias voltage and tip−surface separation.[54] Various types of defects are present on the surface. The bright features (marked with white circles) located on the oxygen rows are most likely hydroxyls, typically 0.7 Å higher than the O_{2c} rows. The dark features (indicated by black circles) are of unknown origin. Sometimes we observe that they become covered by a brighter atom (a hydroxyl group) in consecutive scans. We suspect that these are impurities of the anatase mineral sample. Their concentration is below the detection limit of XPS, but a reasonable guess of their identity would be alkali or alkali earth atoms. These are common impurities in natural anatase minerals and segregate to the surface upon annealing; K atoms appear as dark spots in empty-states STM images of TiO_2 rutile (110).[55] The density of oxygen vacancies is low on well-annealed anatase (101) surfaces; we thus have resorted to creating them by electron bombardment (see below).

Table 1. Calculated Structural Parameters (in Å) and Adsorption Energies (in eV) of Pt and Au Monomers at Terraces, Step D-(112), Step B-(100), and O Vacancy of Anatase TiO_2(101) Surfaces[a]

		M–O_{2c}	M–O_{2c}*	M–Ti	E_a	figure
Pt_1	TiO_2(101)	2.044	2.044	2.780	2.20	Figure 2a
	step D	2.101	2.117	2.443	2.68	Figure 2c
	step B	2.007	2.006	2.643	2.74	Figure 2e
	O vacancy			2.405	4.71	Figure 5a
Au_1	TiO_2(101)	2.358		2.747	0.25	Figure 2b
	step D	2.030	2.004	2.830	0.78	Figure 2d
	step B	2.024	2.025		1.07	Figure 2f
	O vacancy			2.548	3.16	Figure 5d

[a] M indicates the metal (Pt or Au) atom, and O_{2c}, O_{2c}*, and Ti are the O and Ti atoms the metal atoms directly binding with. In the case of steps, O_{2c} and O_{2c}* refer to the O atoms at upper and lower terraces, respectively.

Also marked on Figure 1e are the two types of step edges considered in the calculations. The structure of step D-(112) is consistent with the computed one (Figure 1c);[47] sometimes, additional bright adsorbates are located along these step edges. Step B-(100) appears with two terminations of roughly equal occurrence. The straight parts are consistent with the unreconstructed step edge in Figure 1d. Other parts are decorated with additional features that have a 1 × 3 periodicity. We tested whether these periodic features could possibly be ordered arrays of water molecules or hydroxyls, as our previous work has shown that step edges are quite reactive.[47] However, purposely exposing the surface to water/heating the sample in oxygen did not lead to addition/removal of these features. A step edge reconstruction, or added TiO_x features that grow at the step edges during our sputtering/annealing preparation procedure, appears to be a likely cause for these features, which was not considered in the calculations.

3.2. Calculations of Pt and Au adsorption on terraces and steps of stoichiometric anatase TiO_2(101). 3.2.1. Pt_1 and Au_1. Our results for the adsorption of single Pt and Au atoms are summarized in Figure 2, showing the optimized structures, and Table 1, providing relevant structural parameters and adsorption energies. The preferential adsorption site for a Pt atom on "flat" anatase TiO_2(101) is a highly

(54) DiValentin, C.; Dulub, O. In preparation.
(55) Pang, C. L.; Muryn, C. A.; Woodhead, A. P.; Raza, H.; Haycock, S. A.; Dhanak, V. R.; Thornton, G. *Surf. Sci.* **2005**, *583*, L147.

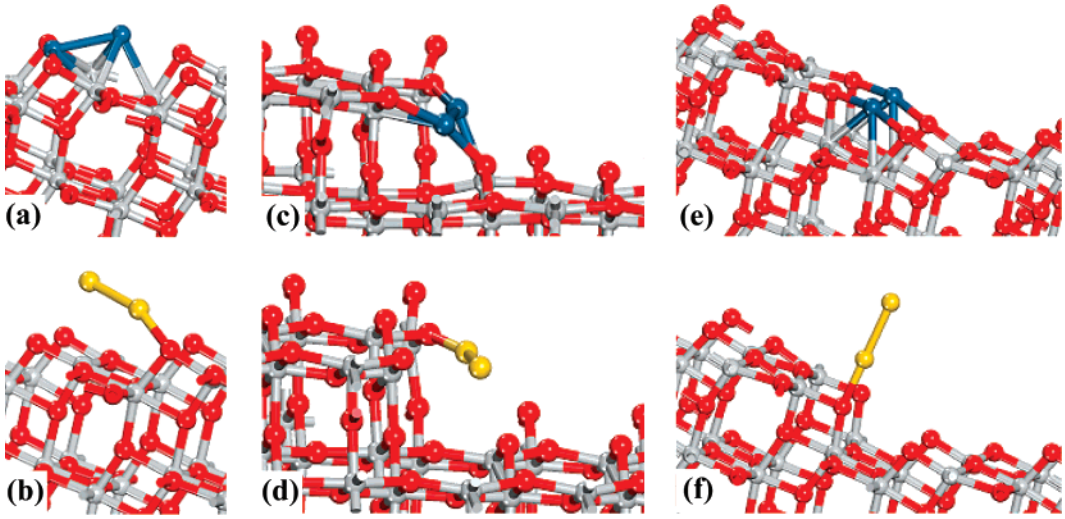

Figure 3. Calculated structures of adsorbed Pt/Au dimers at (a)/(b) terraces, (c)/(d) step D-(112), and (e)/(f) step B-(100) of anatase TiO_2(101) surfaces.

coordinated site in between two O_{2c} and close to two Ti_{5c} and two Ti_{6c} surface atoms, with average Pt−O_{2c} and Pt−Ti distances of ∼2.04 and 2.78 Å, respectively (see Figure 2a). The high coordination of the adsorbed Pt indicates a strong interaction with the anatase surface. Indeed, the adsorption energy is quite large, 2.20 eV. At variance with Pt, the Au atom prefers to sit ∼ 2.75 Å above a single Ti_{5c}, the closest oxygen being a nearby O_{2c} at a distance of ∼2.36 Å (see Figure 2b). This structure suggests that the interaction of Au_1 with the anatase surface is weak, consistent with the calculated adsorption energy of only 0.25 eV. Altogether, our calculations for Au_1/TiO_2 and Pt_1/TiO_2 are in agreement with previous theoretical studies.[42−44] Interestingly, our computed Au_1 adsorption energy is also similar to the values obtained in recent theoretical studies for a gold monomer on the stoichiometric rutile TiO_2(110) surface.[23,30] We notice, however, that the Pt_1 adsorption energy on stoichiometric anatase TiO_2(101) obtained in refs 43 and 44 (2.8 eV) is somewhat higher than our value of 2.2 eV, which may be due to the different surface cell and GGA functional used in the current work.

At step D-(112), Pt_1 binds to two O_{2c}, both at distance of ∼2.1 Å, one at the step edge and the other on the terrace below, and with one Ti_{5c} on the lower terrace (Figure 2c). The Pt−Ti_{5c} bond length, ∼2.44 Å, is much shorter than the Pt−Ti_{5c} distance on the (101) terrace, which may explain why the calculated adsorption energy at step D-(112), 2.68 eV, is ∼22% higher than that on the terrace (2.20 eV). A similar adsorption energy, 2.74 eV, is found also at the B-(100) step, where the Pt atom binds with two O_{2c} (bond lengths of ∼2.0 Å), one at the step edge and the other on the lower terrace, and two Ti_{6c} (bond lengths of ∼2.6 Å) (see Figure 2e).

Similarly to Pt_1, a Au monomer at step D-(112) also binds to two O_{2c}, one at the step edge and the other on the lower terrace, and to the terrace Ti_{5c} atom as well (see Figure 2d). However, surface atoms are found to rearrange significantly upon Au_1 adsorption; the terrace O_{2c} atom binding with the Au monomer actually breaks the bond with the Ti_{6c} below. The average Au−O_{2c} distance is about 2 Å, while the Au−Ti_{5c} distance is 2.83 Å, similar to that on a terrace. The Au_1 adsorption energy at step D-(112), 0.78 eV, is much higher than that, 0.25 eV, on a terrace, indicating that step D-(112) is much more favorable for Au_1 adsorption. Note that although Pt_1 also adsorbs more strongly at step D-(112) than on a (101) terrace, the adsorption energy change for Pt_1 is relatively much less important than that for Au_1. This suggests that D steps should have a much more important role in the adsorption of Au than in that of Pt atoms. At the B-(100) step, the Au monomer binds with two O_{2c} (at distances of ∼2.0 Å) and has almost no interaction with Ti atoms (see Figure 2f). The calculated adsorption energy for Au_1, 1.07 eV, is much higher than the Au adsorption energy on (101) terraces and also about 40% higher than that at step D-(112).

Table 2. Calculated Structural Parameters and Adsorption Energies of Pt and Au Dimers at Terraces, Step D-(112), Step B-(100), and O Vacancy of Anatase TiO_2(101) Surfaces[a]

		M–M	M–O_{2c}	M–Ti	$E^{ads}_{M_2}$		$E^{coh}_{M_2}$figure
Pt_2	TiO_2(101)	2.640	2.049	2.726	1.87	2.52	Figure 3a
	step D	2.659	2.100	2.518	2.32	2.74	Figure 3c
	step B		2.013	2.682	2.11	2.64	Figure 3e
	O vacancy	2.515	2.091	2.544	4.52	3.84	Figure 5b
Au_2	TiO_2(101)	2.493	2.082	2.983	0.98	1.68	Figure 3b
	step D	2.499	2.100	2.852	1.06	1.71	Figure 3d
	step B	2.486	2.082		1.02	1.68	Figure 3f
	O vacancy	2.710		2.623	2.41	2.47	Figure 5e

[a] For the Pt dimer, M−O_{2c} and M−Ti are the average distances between the two Pt atoms of the dimer and their closet O and Ti atoms, respectively. For the Au dimer, M−O_{2c} is the length of the single Au−O bond and M−Ti is the distance between the terminal Au without direct contact with the surface and the nearest Ti.

In general, by comparing the adsorption of Pt_1 and Au_1 on (101) terraces and steps, we can conclude that, while steps are favored for the adsorption of both metal monomers, the step promotion effect is more significant for Au_1 than for Pt_1.

3.2.2. Pt_2 and Au_2. The most stable adsorption structures of Pt and Au dimers are shown in Figure 3, while structural parameters and adsorption energies are reported in Table 2. For Pt_2 on the flat anatase (101) surface (Figure 3a), one of the Pt atoms of the dimer is at almost the same site as a single Pt_1, while the other Pt atom binds with both the first Pt (Pt−Pt distance of ∼2.64 Å) and three surface Ti atoms (Pt−Ti distances of ∼2.7 Å). The adsorption energy per Pt atom, $E^{coh}_{Pt_2}$ = 2.52 eV (see Table 2), is higher than that of a Pt monomer (2.20 eV), indicating that a second Pt atom arriving on the surface prefers to bind to an already adsorbed Pt atom rather than to a surface site far away.

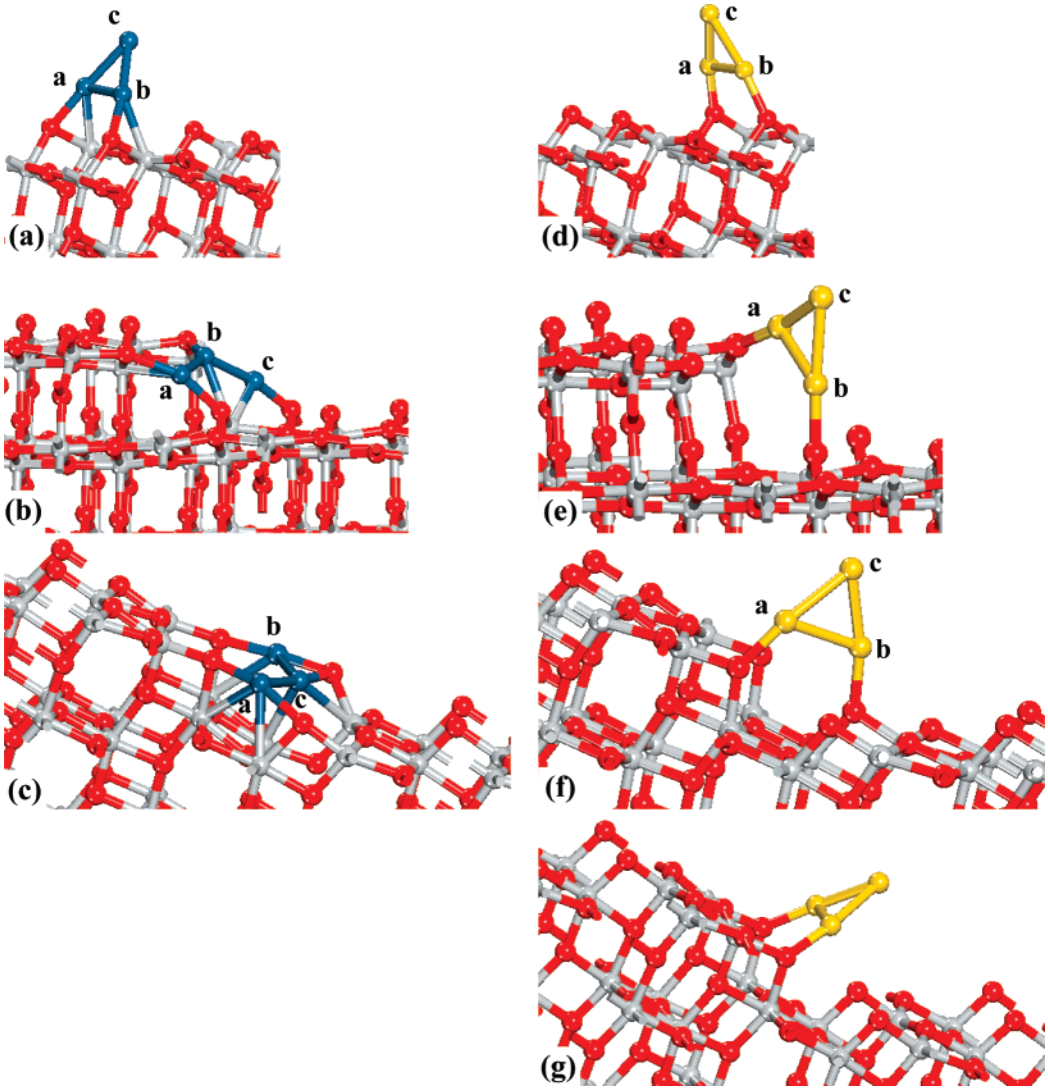

Figure 4. Calculated structures of adsorbed Pt/Au trimers at (a)/(d) terraces, (b)/(e) step D-(112), and (c)/(f, g) step B-(100) of anatase TiO_2(101) surfaces.

Table 3. Calculated Structural Parameters and Adsorption Energies of Pt and Au Trimers at Terraces, Step D-(112), Step B-(100), and O Vacancy of Anatase TiO_2(101) Surfaces[a]

		M–M	M–O_{2c}	M–Ti	$E^{ads}_{M_2}$	$E^{coh}_{M_2}$	figure
Pt_3	TiO_2(101)	2.496	2.061	2.672	2.75	2.94	Figure 4a
	step D	2.653	2.103	2.639	2.45	2.84	Figure 4b
	step B	2.599	2.045	2.751	2.61	2.89	Figure 4c
	O vacancy	2.629	2.153	2.621	5.05	3.71	Figure 5c
Au_3	TiO_2(101)	2.617	2.049		1.63	1.79	Figure 4d
	step D	2.611	2.051		1.87	1.87	Figure 4e
	step B	2.606	2.038		1.82	1.85	Figure 4f
		2.617	2.061		1.79	1.84	Figure 4g
	O vacancy	2.559		2.770	3.10	2.30	Figure 5f

[a] M−M is the average Pt−Pt or Au−Au bond length. For the Pt trimer, M−O_{2c} and M−Ti are the average distances between the trimer atoms and corresponding surface atoms they bind to. For the Au trimer, only average Au−O_{2c} (Au−Ti) bond lengths are given for structures at stochiometric surfaces (O vacancy).

Unlike Pt_2, the gold dimer interacts with the (101) surface mainly through a single, rather short (∼ 2 Å) Au−O_{2c} bond (see Figure 3b). The Au−Au bond length is ∼2.49 Å (vs 2.497 Å in gas phase). The average adsorption energy per Au atom, $E^{coh}_{M_2}$ = 1.68 eV, is much higher than that of Au_1. This increase originates from the Au−Au interaction and indicates a strong tendency for this metal to form aggregates on the surface. Comparison of our Au_2 adsorption/desorption energy ($E^{ads}_{M_2}$ in Table 2) to recent calculations for gold clusters on stoichiometric rutile (110) shows good agreement with the results of ref 30 (see also ref 56), whereas the Au_2 adhesion energy reported in ref 23 appears to be substantially smaller.

At step D-(112), one Pt of the Pt_2 dimer has a position similar to that of Pt_1 in Figure 2c, while the other Pt binds with the O_{2c} atoms at the step edge and terrace and the Ti_{5c} at the edge (see Figure 3b). The Pt−Pt distance, ∼2.66 Å, is close to that on the (101) terrace, and the computed average adsorption energy per Pt atom, 2.74 eV, is only slightly higher than the adsorption energy, 2.68 eV, of Pt_1 at step D-(112). For Au_2, the optimized structure at step D-(112) is similar to that on the (101) terrace (see Figure 3d). In particular, also at step D-(112) Au_2 adsorbs mainly through one Au−O_{2c} bond, and it interacts with other surface atoms very weakly. The Au−Au distance, ∼2.50 Å, is almost identical to that of the dimer on the (101) terrace, and the adsorption energy per Au atom, 1.71 eV, is very similar as well.

Results for Pt_2 and Au_2 adsorption at step B-(100) confirm that Pt_2 interacts much more strongly with the surface than Au_2.

(56) Chretien, S.; Metiu, H. *J. Chem. Phys.* **2007**, *127*, 149902.

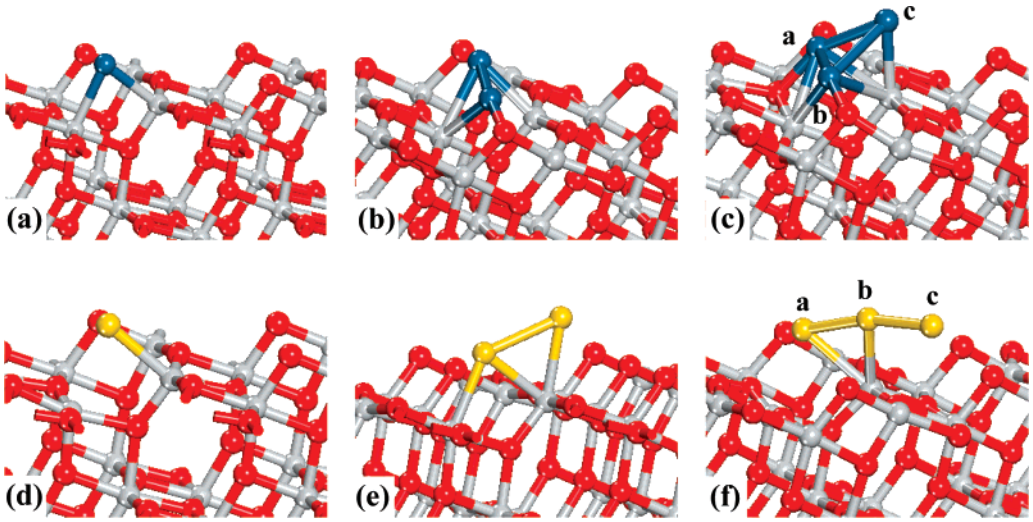

Figure 5. Calculated structures of adsorbed Pt/Au (a)/(d) monomer, (b)/(e) dimer, and (c)/(f) trimer at the O vacancy of anatase TiO_2(101) terraces.

In fact, Pt_2 is *dissociatively* adsorbed at the B-(100) step edge (see Figure 3e), and the average adsorption energy per Pt atom, 2.64 eV, is even slightly smaller than that of a Pt monomer (2.74 eV). Thus formation of a Pt dimer is unfavorable at step B-(100). By contrast, the two Au atoms of Au_2 are strongly bonded together at step B-(100), and Au_2 forms only one bond with a surface O_{2c} at the step edge, similar to the case on a (101) terrace and at step D-(112). The average adsorption energy per atom, 1.68 eV, is also similar to that of the Au dimer at other sites.

3.2.3. Pt_3 and Au_3. For Pt and Au trimers, the most stable adsorption configurations are shown in Figure 4, while structural parameters and adsorption energies are given in Table 3. Pt_3 adsorbed on the flat (101) surface takes a triangular configuration with nearly identical Pt−Pt bond lengths of ∼2.50 Å (Figure 4a). Only two Pt atoms of the trimer form bonds with the surface. The average adsorption energy per Pt atom, 2.94 eV, is 0.74 and 0.42 eV higher than that of the monomer and dimer, respectively. This indicates that three-dimensional (3-D) growth of the clusters is favored on (101) terraces. Similar results hold also for Au_3 (see Figure 4d), with an average adsorption energy per Au atom, 1.79 eV, 0.11 eV higher than that of supported Au_2. Our results for the gold trimer on the anatase surface are also qualitatively similar to those for Au_3 on rutile (110) (see, e.g., refs 23 and 30).

By contrast, the most stable structure for a Pt_3 cluster at step D-(112) (see Figure 4b) is a "lying" (or "2D") structure. This can be obtained by adding an extra Pt atom to one side of the dimer shown in Figure 3c; the extra Pt atom is also bonded with Ti_{5c} and O_{2c} atoms on the lower terrace. The distance between the extra Pt and the Pt it attaches to is 2.62 Å, while that between the other two Pt atoms is 2.68 Å. A 2D structure for Pt_3 is also found at step B-(100), where all the three Pt atoms are directly bonded with Ti_{5c} and O_{2c} atoms at the step edge (see Figure 4c). The Pt−Pt distances are 2.52 and 2.67 Å. The Pt−Pt bond lengths for Pt_3 at steps are similar to those of dimers at (101) terraces and steps but significantly longer than the Pt−Pt bond length (∼2.50 Å) for Pt_3 on a (101) terrace. Indeed, Pt atoms in the 2-D trimers at steps have stronger interactions with the surface than the Pt atoms in the 3-D clusters on terraces. This difference is also reflected in the average adsorption energy per atom, which is 2.94, 2.84, and 2.89 eV for Pt_3 on a (101) terrace, at step D-(112) and at step B-(100), respectively. The higher adsorption energy for Pt_3 on terraces than at steps can be also attributed to the different, 3D vs 2D, structure for the two cases.

The most stable Au_3 structures at terraces and steps are shown in Figure 4d−f (at step B-(100), two structures with very similar stabilities are found). In all cases Au_3 takes a triangular conformation, in which two Au atoms bind with two surface O_{2c} and the third Au atom sits above the first two and has no contact with the surface. The structural parameters (Au−Au and Au−O_{2c} distances) and adsorption energies for the adsorbed trimers are also very similar in the various cases.

3.3. Calculations of Adsorption on the Partially Reduced Anatase (101) Surface. There is experimental evidence that the concentration of surface oxygen vacancies on anatase TiO_2-(101) is significantly lower than on the more extensively studied rutile TiO_2 (110) surface.[57] This is supported by the calculated vacancy formation energy of 4.81 eV, about 1 eV higher than that on the rutile (110) surface.[58,59] Still, it is interesting to study the adsorption of metal clusters at vacancy sites of anatase TiO_2-(101) in order to obtain a comprehensive understanding of the role of different surface sites in the nucleation and growth of supported metal particles.

The most favorable adsorption structures of Pt and Au monomers, dimers, and trimers on partially reduced anatase (101) are presented in Figure 5, and their structural parameters and calculated adsorption energies are listed in Tables 1−3. From these results, we can see that a single Pt atom prefers to adsorb at the position of the missing O_{2c} and binds to the two neighboring Ti_{v-5c} and Ti_{v-4c} only, with bond lengths of ∼2.46 and 2.34 Å, respectively. The computed adsorption energy, 4.71 eV, is much higher than the value obtained for the stoichiometric surface. When another Pt atom is added, the preferred structure has the second Pt atom inserted in between the first Pt at the vacancy site and one O_{2c} nearby, forming a linear structure, with Pt−Pt and Pt−O_{2c} distances of ∼2.51 and 2.09 Å, respectively (Figure 5b). The adsorption energy per Pt atom,

(57) Herman, G. S.; Dohnálek, Z.; Ruzycki, N.; Diebold, U. *J. Phys. Chem. B* **2003**, *107*, 2788.
(58) Wu, X.; Selloni, A.; Lazzeri, M.; Nayak, S. K. *Phys. Rev. B* **2003**, *68*, 241402.
(59) Rasmussen, M. D.; Molina, L. M.; Hammer, B. *J. Chem. Phys.* **2004**, *120*, 988.

Table 4. Calculated Lowdin Charges (in *e*) of Each Pt (Au) Atoms in the Adsorbed Pt (Au) Trimer at Terraces, Step D-(112), Step B-(100), and O Vacancy of Anatase TiO_2(101)[a]

	Pt_a	Pt_b	Pt_c	figure	Au_a	Au_b	Au_c	figure
(101)	0.99	0.99	0.69	Figure 4a	0.06	0.06	0.12	Figure 4d
D-(112)	1.02	1.03	0.97	Figure 4b	0.07	0.04	0.16	Figure 4e
B-(100)	1.11	1.05	1.01	Figure 4c	0.07	0.08	0.14	Figure 4f
O vacancy	0.96	0.94	0.78	Figure 5c	0.01	−0.15	−0.04	Figure 5f

[a] The specific atoms are labeled in the corresponding figures.

3.84 eV, is also higher than that on the stoichiometric surface and in good agreement with recent calculations by Iddir et al.[44] For Pt_3, numerous structures with both 2-D and 3-D character were tested. The preferred one turns out to be the 3-D conformation shown in Figure 5c. By comparing the trimer and dimer structures, we can see that the evolution from the dimer to the trimer proceeds through the addition of a third Pt atom above the dimer, giving rise to a triangular structure. At variance with the triangular Pt_3 cluster at terraces, shown in Figure 4a, all three Pt atoms now bind with the surface via multiple Pt−Ti and Pt−O bonds at the vacancy site. This may explain why the average Pt−Pt bond length (2.63 Å) is relatively longer than that at terraces (2.50 Å). The calculated average adsorption energy is 3.71 eV, which is still higher than that of trimers on stoichiometric surfaces.

The adsorption of Au_n ($n = 1-3$) clusters on partially reduced anatase TiO_2(101) has been studied by our group a few years ago.[42] In the present work, we confirmed those results by repeating the calculations for some key structures (see Figure 5d−f). On the partially reduced surface the Au_3 cluster is almost linear, at variance with the structures of Au_3 at terraces and steps. As for the Pt_n clusters, the calculated adsorption energies for Au_n at the vacancy site are much higher than those for the stoichiometric surfaces. For example, the Au monomer, which binds to a single Ti_{v-4c} at the vacancy site, has an adsorption energy as high as 3.16 eV, indicating that Au preferentially nucleates at vacancy sites.

3.4. Calculation of Charge Transfers between the Supported Metal Clusters and the Anatase Surface. In an attempt to elucidate the origin of the enhanced activity of oxide-supported metal catalysts, it has been proposed that an important role is played by the charge state of the supported metal clusters.[60] In this context, it is interesting to determine how the charge state of the cluster changes at different adsorption sites. For this reason we have calculated the Lowdin charges of the metal atoms in the supported Pt and Au trimers on different surfaces (see Table 4). Lowdin charges (obtained by integrating the electronic density of states projected onto atomic states centered at the various atoms) are not quantitatively meaningful, but trends in their relative values provide useful qualitative information. We can see that, compared to stoichiometric (101) terraces, steps and O vacancies affect the charges of Pt and Au trimers in very different ways. Pt_3 adsorbed at steps is significantly more positive than that on (101) terraces, whereas, somewhat surprisingly, there is no significant change in the total charge when Pt_3 is adsorbed at an O vacancy. This suggests that the (occupied) electronic states associated to the oxygen vacancy are lower in energy than the lowest available (i.e., empty) states associated to the Pt cluster, so that no charge transfer from the vacancy to the cluster can occur. By contrast, while the charge distributions for Au_3 at steps and terraces are very similar, O vacancies have a remarkably strong effect on the charge distribution and change the overall charge of the Au cluster from positive (+0.24 *e* on a terrace) to negative (−0.18 *e*); i.e., the negative charge is transferred from the vacancy to the cluster. This result suggests that the properties of Au clusters would be very sensitive to the nucleation site, and small clusters at O vacancies may exhibit quite different properties compared to those at terraces and step edges.

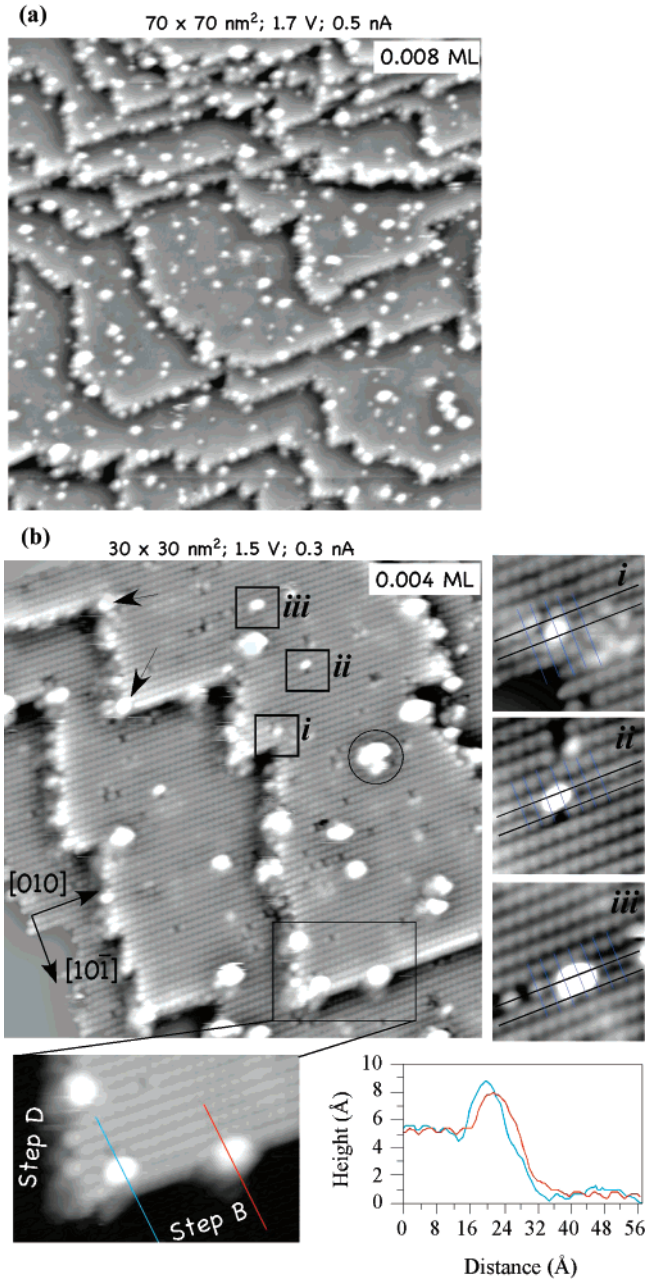

Figure 6. (a) Overview STM image of a sputtered/annealed anatase(101) surface after deposition of 0.008 ML of Pt. (b) Smaller-scale STM image with 0.004 ML Pt on anatase (101). The inset and line profiles at the bottom show that Pt clusters at step edges are mostly located at the upper terraces. Kink sites are preferred nucleation sites (see black arrows in (b)). The clusters in the enlarged areas (*i*−*iii*) are tentatively assigned as a (i) Pt monomer, (ii) Pt dimer, and (iii) Pt trimer.

3.5. STM of Pt Deposited on Anatase (101). Figure 6 shows STM images of the sputtered/annealed surface after deposition

(60) Wang, J. G.; Hammer, B. *Top. Catal.* **2007**, *44*, 49.

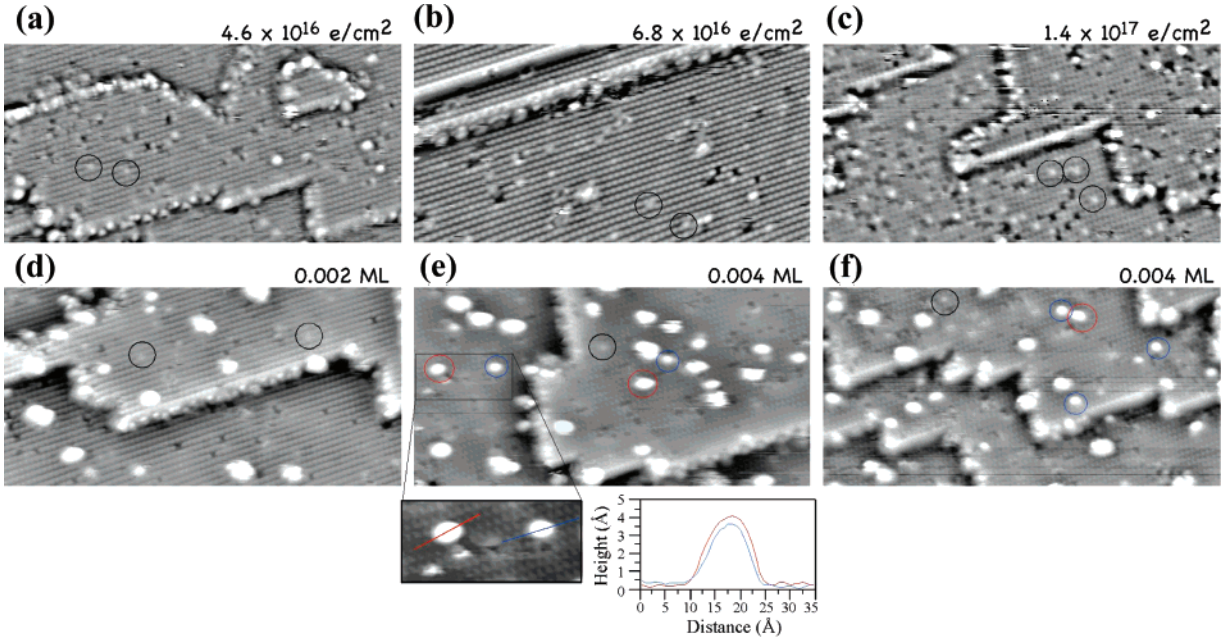

Figure 7. STM images after irradiation with 300 eV electrons at fluences of (a) 4.6×10^{16}, (b) 6.8×10^{16}, and (c) 1.4×10^{17} e/cm^2. Oxygen vacancies are marked with black circles. The images in (d−f) show the surfaces from (a−c), respectively, after vapor-depositing Pt with coverages of (d) 0.002 ML and (e, f) 0.004 ML.

of small amounts of Pt (0.004−0.008 ML). Pt clusters appear to be homogeneously distributed on the surface. A statistical evaluation (not shown here) indicates that the clusters' height increases with coverage, which is characteristic for 3D cluster growth.[61] The Pt clusters at terraces in Figure 6b are ∼2.3−5.7 Å high and ∼5−14 Å wide; larger clusters are elongated along the [010] direction. The wide size distribution indicates nucleation of the Pt clusters at special surface sites; it is difficult to determine the reason(s) for nucleation at the terraces experimentally. We can exclude the black impurity spots as trapping sites as these often remain unpopulated next to clusters. The clusters are fairly stable and immobile under the tunneling conditions given in Figure 6. When purposely increasing the sample current to 3 nA, some clusters could be removed (not shown here). The undisturbed lattice became visible, with no apparent special site at the former position of the cluster. However, an adsorbate that was originally responsible for a cluster to nucleate at that site may have been swiped away as well.

It is generally hard to determine the exact size of very small supported clusters with STM because of tip convolution and electronic structure effects, which affect their width and apparent height, respectively, in atomically resolved STM images. The assignment of small clusters (Figure 6) was based on the observation that the smallest clusters had a similar (monoatomic) height and showed a monotonic increase in width, and by registry of the clusters with the anatase lattice. The three panels (i−iii) at the right side of Figure 6b show some of the smallest clusters that were observed, the black/faint blue lines in the images marking the registry with the O_{2c} atoms along the [010]/[101] directions. The smallest cluster (2.3 Å high and 3.5 Å wide) marked with (*i*) is then tentatively attributed to a Pt monomer. Its center is located at the rows of O_{2c} atoms, slightly shifted toward the neighboring Ti_{5c}. Its maximum is located on top of an O_{2c} site. The center of the next biggest cluster (*ii*) (2.5 Å high and 5 Å wide) is shifted closer to the Ti_{5c} rows (in the downward direction from atomic rows in the STM images). We tentatively assign this cluster as a dimer. The next bigger cluster in this series (*iii*) appears as 2.7 Å high and 8 Å wide and is now clearly elongated along the rows; this might be a flat-lying trimer. The calculations (Figure 4a) predict that, in the lowest-energy configuration, the third Pt atom is located above the first two Pt atoms. In addition to these flat trimers, we do observe clusters that have a width that is in between those of the flat dimers and trimers but with a larger height; for example, the cluster located close to step B, marked with a blue line, sits 3.3 Å above the terrace. Note that this cluster is now centered on top of an O_{2c} row, which would indicate that differently shaped trimers have different nucleation sites.

Although some bonding occurs at step edges, there is no clear preference for steps as nucleation sites. Kinks, however, are quite frequently populated (arrows in Figure 6b). Many clusters next to step edges are located at the upper terrace (see the line profiles of the Pt clusters shown in Figure 6b). Nucleation at an upper terrace is often considered an indication for a high Schwoebel−Ehrlich barrier that prevents the atoms from stepping down toward the lower terrace.

It is well-established that irradiation of TiO_2 with electrons causes the desorption of oxygen;[10] the resulting oxygen vacancies have started to be investigated with STM only recently.[48] Figure 7a shows the effect of electron irradiation on anatase (101). Bright spots (marked as dark circles in Figure 7) appear, which are slightly offset from the O_{2c} rows. The density of these bright spots increases with electron fluence (see Figure 7a−c). The appearance of O_{vac} as bright spots is in agreement with Tersoff−Haman calculations.[62] The Pt cluster density and size are similar to those for the clean, annealed anatase (101) surface (compare Figures 6b and 7d); some O_{vac} sites remain unoccupied, even if they are located in the immediate neighborhood

(61) Chen, D. A.; Bartelt, M. C.; Hwang, R. Q.; McCarty, K. F. *Surf. Sci.* **2000**, *450*, 78.

(62) Finazzi, E.; Di Valentin, C.; Selloni, A.; Pacchioni, G. *J. Phys. Chem. C* **2007**, *111*, 9275.

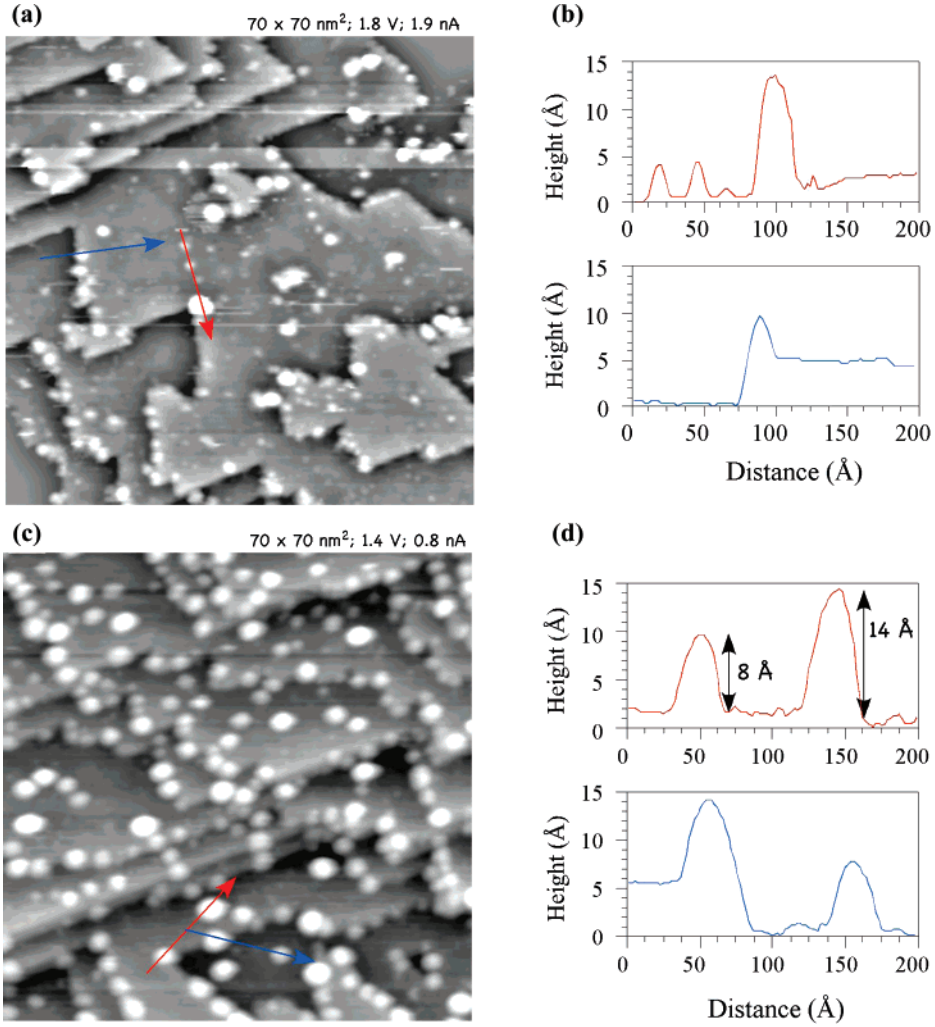

Figure 8. STM images for (a) 0.009 ML and (c) 0.06 ML Au on the anatase (101) surface prepared by sputtering and annealing as in Figure 1e. (b) and (d) Line profiles of 3D clusters on the terraces and the step edges.

of an existing cluster. This is also true for higher electron dosages (Figure 7c and f), where the surface becomes visibly damaged. A closer analysis of the location of small clusters shows a higher propensity for the smaller clusters being centered on O_{2c} rows, however. For example the two clusters pointed out in red and blue in the inset of Figure 7e are probably trimers that have nucleated at an O_{vac} site.

3.6. STM of Au Deposited on Anatase (101). Figure 8 shows STM images of the annealed surface with increasing Au coverage. Imaging Au-covered surfaces was challenging, possibly due to mobile Au that is present at the surface at room temperature. The clusters grow in size, from ~3.2−4.3 Å high and 4−10 Å wide in Figure 8a to clearly three-dimensional in Figure 8c. The growth behavior is more 3D-like than that for Pt (compare Figures 6 and 8). A few clusters nucleate at terrace sites, but it was difficult to determine their exact size and registry with the anatase lattice. At variance to the behavior of Pt, however, a clear preference for nucleation at step edges is observed. Interestingly, steps D-(112) are more populated with clusters than type B-(100) steps. The total energy calculations do not predict such a behavior; it is likely that kinetic effects are the reason for this preference. For oxide systems with anisotropic diffusion, clusters tend to nucleate at step edges that cut across the fast diffusion direction.[49,63] For the anatase (101) case, we expect that motion will occur more readily along the [010] direction, parallel to the O_{2c} rows, providing for a metal flux toward the type D-(112) steps. As has already been seen for Pt, kink sites distinguish themselves as positions where large clusters are present at smaller coverages.

Oxygen vacancies have a marked effect on the growth of Au on anatase (101) (see Figure 9). The Au coverages and image sizes in Figures 8c and 9b are similar, yet the cluster size and distribution are strikingly different. The clusters on the electron-irradiated surface in Figure 9 are much smaller and scattered across the whole terrace, with very few located at the step edges. For lower coverages very small clusters are observed that are located at the O_{2c} rows (Figure 9a, blue circle in the inset); we tentatively assign these as Au monomers at vacancy sites. A similar effect has recently been observed for Au/rutile (110);[23] where Au nucleated at terraces on a reduced surface, and on a surface where O adatoms were created by exposure of the reduced surface to molecular oxygen. When the oxygen vacancies were saturated with surface hydroxyls, Au nucleated preferentially at step edges. A comparison of the results of

(63) Dulub, O.; Boatner, L. A.; Diebold, U. *Surf. Sci.* **2002**, *519*, 201.

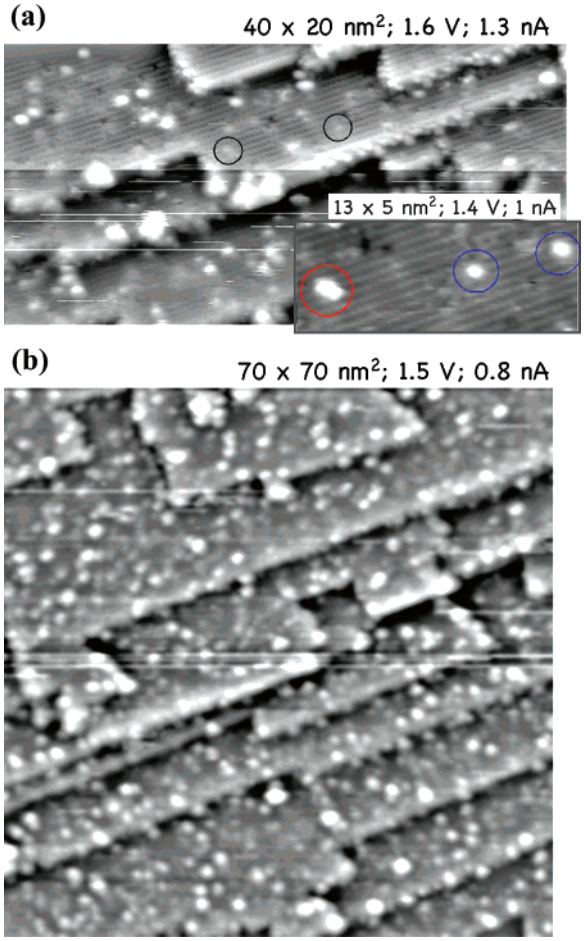

Figure 9. STM images of the electron irradiated surface (300 eV, 1.4×10^{17} e/cm^2) after deposition of (a) 0.005 ML (b) and 0.06 ML of Au. Circles in (a) indicate oxygen vacancies (black) and Au monomers (blue) and larger Au clusters (red).

Matthey et al. and the data shown here suggests that the nucleation behaviors are similar on the two TiO_2 polymorphs.

4. Discussion

Our STM results not only confirm many of the theoretical results but also point out the difficulty of directly comparing total-energy calculations of various adsorbate configurations with growth experiments, where surfaces are even more inhomogeneous than the well-defined defects considered here and kinetic effects play a role.

Our calculations show that single Pt and Au atoms have higher adsorption energies at B-(112) and D-(100) steps than on the (101) terrace. For Pt, the adsorption energy increase at the steps is just about 20%, but for Au the increase is by a factor of 3−4, from as low as 0.25 eV on the terrace to 0.78 and 1.07 eV at step D-(112) and B-(100), respectively. When a second metal atom is adsorbed on (101) terraces, the formation of dimer species is always favored with respect to the adsorption of separate monomers. This is especially evident for Au but holds also for Pt. At the steps, the behaviors of Pt and Au become somewhat different. For Pt at the steps, dimer species are only marginally more stable at step D-(112) or even slightly less stable at step B-(100) than separate monomers, even though adsorption at the steps is still somewhat preferred with respect to adsorption on terraces. For Au, dimerization is always favored, but dimers at steps are essentially as stable as those on terraces. The stability of the dimers comes indeed from the strength of the Au−Au bond, as suggested also by the characteristic adsorption structures, where only one Au atom interacts strongly with the surface.

Turning next to trimers, our calculations indicate that Pt_3 prefers to take a "standing" (or "3-D") conformation on (101) terraces, while at both steps D-(112) and B-(100) it stretches along the edges forming 2-D structures. Interestingly, the calculated Pt_3 adsorption energy turns out to be higher at terraces than at steps, likely because the strong Pt−Pt interactions are better optimized in the 3D structure at terraces. Therefore, although steps have a slightly stronger affinity than (101) terraces for Pt monomers and dimers, they actually seem to be less favorable for the growth and adsorption of bigger clusters. In other words, larger Pt clusters prefer to have a 3-D conformation and to be located on terraces. This is consistent with the STM observation that Pt clusters are largely located on (101) terraces and do not show any preference to be at steps.

Unlike Pt trimers, Au_3 clusters are predicted to have similar 3-D structures at terraces and steps. Adsorption at steps is only slightly favored compared to adsorption on terraces, as the cluster stability is essentially determined by Au−Au and not by Au−surface interactions. Thus, while Au nucleation (monomer adsorption) at the steps is strongly preferred with respect to adsorption at (101) terraces, our computed adsorption energies suggest that Au clusters may not remain at the steps during growth. On the other hand, experimentally, nucleation at defects in combination with a distribution of nucleation sites leads to a range of cluster sizes even for the smallest coverages. This prevents us from following the predicted change in site preference that is expected from the total-energy calculations.

The STM results are very much in line with the larger adsorption energy of Pt as compared to Au. Smaller Pt clusters with a less pronounced 3D growth are observed for comparable metal coverages on similarly prepared surfaces. Pt clusters as small as monomers are observed. Our images suggest that their position is on top of a O_{2c} site (Figure 6b(i)) rather than in between two O_{2c} atoms (Figure 2a), probably because monomers are not stable on the nondefective surface at room temperature and the ones that are observed are trapped at special nucleation sites. The position of dimers (Figure 6b(ii)) is consistent with the calculations. For Pt trimers various configurations are observed, possibly again because of different nucleation sites (Figure 5a). Au grows in much larger clusters starting from the smallest coverage; thus the preference for different adsorption sites could not be tested on the well-annealed surface. The influence of step edges is much more pronounced than that for Pt.

Although the concentration of O vacancies on well-annealed anatase TiO_2(101) is quite low,[57] both the calculation and the experimental results show that they still play an important role in the nucleation and growth of metals on the (101) surfaces. In fact, Pt_n (Au_n) clusters adsorbed at O vacancies are more than 2 (1) eV more stable than the corresponding clusters on stoichiometric surfaces, according to our calculations. This suggests that whenever O vacancies are present on the surface, they will become the preferred nucleation and growth sites for the metal clusters. The experimental results show a striking

difference between Au and Pt on surfaces with purposely created O vacancies: whereas the Pt cluster sizes and distribution are hardly affected, the influence of vacancies on Au is very pronounced and Au clusters as small as one atom were observed at room temperature. A strong influence of surface oxygen vacancies on Au cluster nucleation and distribution has been also observed in a recent STM study of gold on the rutile TiO_2-(110) surface.[23]

Our results also suggest that there is a threshold (E^t) for the adsorption energy (E^{ads}) of the cluster such that when $E^{ads} < E^t$, diffusion can easily occur. In contrast, diffusion is largely suppressed when $E^{ads} > E^t$, even if more stable adsorption sites are present. For instance, Pt clusters, which have large adsorption energies on stoichiometric terraces, hardly diffuse toward other more stable adsorption sites, such as O vacancies or steps. For Au monomers and dimers the adsorption energy on stoichiometric terraces is weak (less than 1 eV); thus they easily diffuse to steps and O vacancies, where the adsorption is stronger. For Au clusters, the role of surface morphology is also evident. On the stochiometric surface, Au clusters are numerous at step D-(112) because diffusion is facile along [010]. Cluster adsorption energies at step B-(100) are very similar; however this step is not favored because it runs parallel to the preferred diffusion channel. Even though we observed the above effects at relatively low T, it is possible that similar effects are also present in sintering, one of the most important deactivation mechanisms affecting the lifetime of metal supported catalysts.[64,65]

(64) Min, B. K.; Wallace, W. T.; Goodman, D. W. *J. Phys. Chem. B* **2004**, *108*, 14609.
(65) Wallace, W. T.; Min, B. K.; Goodman, D. W. *J. Mol. Catal. A: Chem.* **2005**, *228*, 3.

5. Summary

We have presented DFT calculations of the structure of small Au and Pt clusters, including monomers, dimers, and trimers, adsorbed at regular and defect sites of the anatase TiO_2(101) surface. In combination with these calculations, we have carried out room-temperature STM measurements of both well ordered and electron-irradiated surfaces on which Au and Pt clusters were deposited by evaporation. Calculations predict 3D-like growth of both Au and Pt clusters at clean terraces, which is confirmed by experiment. DFT calculations also indicate that steps and O-vacancies have higher adsorption energies and may act as nucleation sites for Au and Pt growth. These results are only partially confirmed by the STM measurements, which show that steps on clean anatase TiO_2(101), as well as O vacancies on electron-irradiated surfaces, are highly favored by Au clusters, while Pt clusters do not show any preference for growing at these sites. Both energetics and kinetics influence the nucleation and aggregation behavior of the metal clusters. In particular, weakly bonded clusters (Au clusters on clean terraces, for example) are highly mobile, and kinetic effects tend to favor their aggregation at sites with higher adsorption energies through fast diffusion channels.

Acknowledgment. This work was supported by the U.S. Department of Energy (DE-FG02-05ER15702). The authors acknowledge Princeton University (Della and Hecate clusters) and the Department of Chemistry (Eyring cluster) for computing time.

JA0773148